

COMBINED INTENSITY AND COHERENT CHANGE DETECTION FOR SYNTHETIC APERTURE RADAR

Miriam Cha, Rhonda D. Phillips

MIT Lincoln Laboratory
Lexington, Massachusetts 02420 USA
{miriam.cha,rhonda.phillips}@ll.mit.edu

Patrick J. Wolfe

University College London
London WC1E 6BT, UK
p.wolfe@ucl.ac.uk

ABSTRACT

Coherent change detection using paired synthetic aperture radar images is performed using a classical coherence estimator applied under an assumption of complex Gaussian data. The magnitudes of the resulting coherence estimates are plotted as an image and used to gauge changes in the observed scene. In this paper, a two-stage change statistic that combines non-coherent and coherent change detection algorithms is proposed. In the first stage, a non-coherent intensity change detector is applied to test for changes caused by the displacement of a sizable object using the sample variance ratio test. The sample pairs that failed the first stage are used as an input to the second stage. The second stage test uses an alternative coherence estimator that assumes equal population variances, to detect subtle changes such as tire tracks and footprints. We show experimentally that the proposed method not only has a superior change detection performance over the classical coherent change detector, but also over either the non-coherent intensity change detector or the alternative coherent change detector, alone. Experimental results are presented to show the effectiveness and robustness of the proposed algorithm for SAR change detection.

Index Terms— Coherent change detection, interferometric SAR processing, synthetic aperture radar.

1. INTRODUCTION

Synthetic aperture radar (SAR) is an important modality in remote sensing due to its ability to form high resolution images with relative invariance to weather and lighting conditions. SAR images are formed using a moving radar that collects data over a scene from multiple perspectives. The resulting data are complex-valued, with the magnitude corresponding to the reflected signal intensity of the scene and the phase indicating scattering properties.

One application of SAR is change detection, which utilizes two SAR data collections of the same scene at different times to infer changes that have occurred in between data collections. SAR change detection algorithms can be categorized into two: 1) intensity based change detection utilizing local changes in SAR magnitude images to indicate large-scale changes, such as the appearance of a sizeable object during the second collection that was not present during the first; and 2) coherent change detection (CCD) that uses SAR phase as well as magnitude to estimate the coherence between the two SAR

images. CCD requires the two image collections to use identical collection geometries, so that each respective image phase is aligned, leading to the detection of smaller-scale changes.

As [1, 2, 3] have investigated, the traditional coherence magnitude estimator is biased, particularly when the true coherence is small. This bias can be reduced by an increase in the number of samples. However, in practice, there are a limited number of samples to be obtained from each spatial location in a pair of SAR images, as they must be “borrowed” from a local neighborhood or spatial window. As the number of neighboring pixels used to estimate coherence is increased, the effective spatial resolution of the resulting CCD image is decreased, making detection of small-scale changes more difficult. Furthermore, as the size of the sample window increases, the assumption that the samples are drawn independently from the same distribution is less likely to be met. Accurate estimation of coherence from a limited number of samples is a challenging problem, which must be overcome either through better models for the data or more accurate estimators.

Here we adopt the latter approach and introduce a two-stage method that leverages both non-coherent and coherent algorithms for SAR change detection. Traditionally, the classical estimator based on the Pearson correlation coefficient is used for coherence, however, [4] shows that with reasonable assumptions, an alternative coherence estimator yields superior coherence estimation and change detection performance. This coherence estimator assumes both populations have equal variances, which is more likely after the application of the first test. The two-stage method that applies intensity change detection to capture samples with unequal variances prior to application of the alternative estimator is a natural consideration. We show experimentally that the proposed method outperforms not only the classical CCD, but also either the intensity change detector or the alternative CCD, alone.

2. CHANGE DETECTION

SAR data is often modeled as a collection of spatially uncorrelated pixels drawn from a zero-mean circularly complex Gaussian distribution. Given two spatially registered SAR data sets, f and g of N pixels, one can form a joint data vector $X = [f, g]^T \in \mathbb{C}^{N \times 2}$. The N sample pairs $X_k = [f_k, g_k]$, $k = 1, \dots, N$, are viewed as independent samples from a zero-mean, bivariate, complex Gaussian distribution with covariance matrix

$$\Sigma = \mathbb{E}(X X^H) = \begin{bmatrix} \sigma_f^2 & \rho \sigma_f \sigma_g \\ \bar{\rho} \sigma_f \sigma_g & \sigma_g^2 \end{bmatrix}, \quad (1)$$

where

$$\sigma_f^2 = \mathbb{E}(|f|^2), \quad \sigma_g^2 = \mathbb{E}(|g|^2), \quad \rho = \frac{\mathbb{E}(f g^H)}{\sqrt{\mathbb{E}(|f|^2)\mathbb{E}(|g|^2)}}. \quad (2)$$

This work is sponsored by the United States Air Force under Air Force Contract FA8721-05-C-0002. Opinions, interpretations, conclusions and recommendations are those of the author and are not necessarily endorsed by the United States Government. Approved for public release; distribution is unlimited.

Here ρ is the complex correlation coefficient, and $\bar{\rho}$ denotes its complex conjugate. The covariance matrix Σ is typically estimated by the maximum likelihood estimator of the covariance matrix,

$$A = \frac{1}{N} \sum_{k=1}^N X_k X_k^H \equiv \begin{bmatrix} \hat{\sigma}_f^2 & \hat{\rho} \hat{\sigma}_f \hat{\sigma}_g \\ \hat{\rho} \hat{\sigma}_f \hat{\sigma}_g & \hat{\sigma}_g^2 \end{bmatrix}. \quad (3)$$

In practice, A is obtained from spatial neighborhoods of f_k and g_k in the respective SAR images. The following subsections provide a detailed formulation of the non-coherent intensity change detection, the classical coherent change detection and the alternative coherent change detection.

2.1. Non-coherent Intensity Change Detection

Intensity based SAR change detection is often achieved using the result of dividing one magnitude image by the other to identify change as a quotient that significantly deviates from one. Specifically, a variance at one location in f is estimated using a spatial window and the corresponding variance of g is estimated, and the change statistic is

$$\hat{R} = \frac{\hat{\sigma}_f^2}{\hat{\sigma}_g^2}. \quad (4)$$

Values of \hat{R} that differ substantially from one are labeled as change. This statistic is frequently used to test if the underlying variances of two populations are different.

The problem of detecting different sample variances is formulated as a hypothesis test, where the null hypothesis is that the two population variances are equal and the alternative hypothesis is that those populations have different variances. In the absence of correlation, the sample variance ratio \hat{R} has an $F_{2N,2N}$ distribution if the null hypothesis is true, making this test an F -test. If the null hypothesis is true and $\rho = 0$,

$$F(R|H_0) \equiv P(\hat{R} \leq R|H_0) = I_{R/(1+R)}(N, N), \quad (5)$$

where $I_v(a, b)$ is the incomplete beta function [5]. For a chosen test significance level α , we find the upper critical value $R_{u,\alpha}$ and the lower critical value $R_{l,\alpha}$ of the $F_{2N,2N}$ distribution as

$$F(R_{u,\alpha}|H_0) = 1 - \frac{\alpha}{2}, \quad F(R_{l,\alpha}|H_0) = \frac{\alpha}{2}. \quad (6)$$

A sample value \hat{R} such that $\hat{R} < R_{l,\alpha}$ or $\hat{R} > R_{u,\alpha}$ results in the null hypothesis being rejected. When applied to SAR change detection, rejection of the null hypothesis indicates change. This test will reveal large-scale changes that affect SAR magnitude values, such as a car that appears in one image but not another. Smaller scale change detection requires a different change detection method.

2.2. Classical Coherent Change Detection

While non-coherent change detection is generally applicable to any type of real-valued image, coherent change detection requires magnitude and phase. The additional phase data allows smaller scale changes to be detected, such as tire imprints on soft soil. The small ground surface change affects radar scattering, which affects phase. A statistic that is often used to indicate this type of change is coherence, which is estimated using a classical coherence estimator,

$$\hat{\rho}_c = \frac{A_{12}}{\sqrt{A_{11}}\sqrt{A_{22}}}, \quad (7)$$

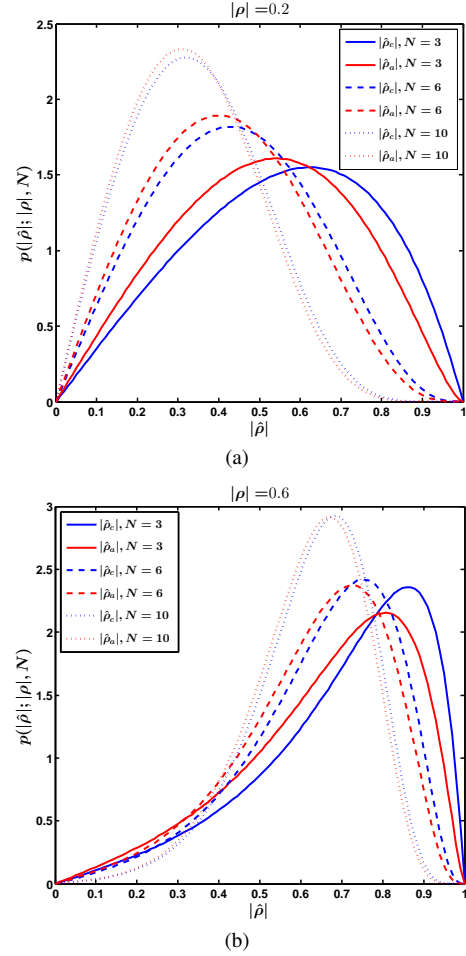


Fig. 1: Sampling distributions of $|\hat{\rho}_c|$ (blue) and $|\hat{\rho}_a|$ (red) shown as a function of sample size N , for true parameter values (a) $|\rho| = 0.2$ and (b) $|\rho| = 0.6$.

(here $\hat{\rho}_c$ denotes the ‘‘classical’’ estimator). This statistic is a random variable that depends on the true underlying coherence $|\rho|$ and the number of samples used in estimation N , and is distributed as

$$p(|\hat{\rho}_c|; |\rho|, N) = 2(N-1)(1-|\rho|^2)^N |\hat{\rho}_c| (1-|\hat{\rho}_c|^2)^{N-2} \cdot {}_2F_1(N, N; 1; |\rho|^2 |\hat{\rho}_c|^2), \quad (8)$$

where ${}_2F_1(\cdot, \cdot; \cdot; \cdot)$ is the Gauss hypergeometric function [1]. Examples of this distribution for different values of $|\rho|$ and N are shown as a blue line in Fig. 1. Notice that the bias of the estimator increases with decreasing $|\rho|$, and is especially pronounced when N is small. This presents a problem in SAR CCD as low coherence values correspond to change, which is what we are trying to detect, and the number of samples available for coherence estimation is small.

Note that as a single pair of SAR images is assumed available, only a limited number of samples is available to estimate coherence. The size of the spatial neighborhood can be increased to increase the effective number of samples. This can have unintended effects of smoothing the eventual CCD image and resulting in missed change detection. However, making an assumption that the underlying population variances remain unchanged will effectively double the number of samples available for estimation.

2.3. Alternative Coherent Change Detection

An alternative coherence estimator, introduced by Berger, provides superior change detection performance assuming variance equality assumptions are met [2]. As change detection requires two SAR images of the same scene, the underlying variances will be equal absent significant changes. When this equal variance assumption is met, the natural estimator of the complex correlation coefficient ρ , denoted $\hat{\rho}_a$, can be written as a function of the elements of A as

$$\hat{\rho}_a = \frac{2 A_{12}}{A_{11} + A_{22}}. \quad (9)$$

Notice that the denominator contains a sum rather than a product of two random variables, suggesting a more stable estimator. Furthermore, since both variance terms are assumed to be equal, the number of samples used to estimate the true variance is effectively doubled. In scenes where most of the underlying variance remains unchanged, this estimator can be expected to offer improved properties over the classical estimator $\hat{\rho}_c$ of (7).

The expression for the probability density function of estimated coherence magnitude $|\hat{\rho}_a|$ is derived by several authors, including in [2]:

$$p(|\hat{\rho}_a|; |\rho|, N) = (2N - 1)(1 - |\rho|^2)^N |\hat{\rho}_a| (1 - |\hat{\rho}_a|^2)^{N - \frac{3}{2}} {}_2F_1(N, N + 1/2; 1; |\rho|^2 |\hat{\rho}_a|^2). \quad (10)$$

Examples of the distribution of $|\hat{\rho}_a|$ for a fixed N and $|\rho|$ are shown in red in Fig. 1. The distribution of $|\hat{\rho}_a|$ appears to have a lower bias and its peak is closer to the true coherence value than the distribution of $|\hat{\rho}_c|$. For large values of N , both probability distributions tend toward $\mathbb{E}[|\rho|]$. These results hint that better estimation is possible using $|\hat{\rho}_a|$ especially when N is limited. Therefore, a two-stage method that applies intensity change detection to capture samples with $\sigma_f \neq \sigma_g$ prior to application of $|\hat{\rho}_a|$ is a natural consideration.

3. TWO-STAGE CHANGE DETECTION

Coherence and intensity ratio statistics are used separately to detect change at different scales, but if change detection, regardless of scale, is the goal, these statistics should be combined to reveal change at all scales. Combining the statistics has the additional benefit of testing first for equal variance, justifying the assumption of equal variance in order to use a more accurate coherence estimator, and in the second step, using the alternative coherence estimator which outperforms CCD that uses $|\hat{\rho}_c|$. The combined test therefore provides superior change detection over either, alone. The procedure for this proposed test is highlighted in Fig. 2. In the next section, the performance of the two-stage detector compared to other detectors is investigated in terms of the receiver operating characteristic (ROC) curves and visual inspection of the change detection images.

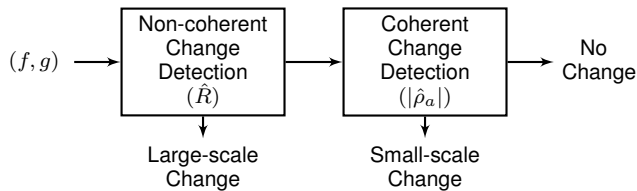


Fig. 2: The block diagram of the two-stage change detection scheme

4. EXPERIMENTAL RESULTS

We performed a simulation with known truth to compare the change detection performance of the two-stage method, $|\hat{\rho}_a|$ and $|\hat{\rho}_c|$. For the purpose of this experiment, $|\rho| = 0$ with a range of values in R was chosen to indicate change, and $|\rho| = 0.9$ with $R = 0.9$ to indicate no effective change. To restrict the unlikely case, the variance ratio R was fixed in generating ‘no change’ samples, and only varied in producing ‘change’ samples. Note that choosing $|\rho| = 1$ or $R = 1$ would result in no variability between samples, which is not realistic in SAR data. Coherence is affected by factors other than scene change, making $|\rho| = 0.9$ a reasonably high coherence value. Results in detecting change corresponding to $|\rho| = 0$ with a range of values in R versus $|\rho| = 0.9$ with $R = 0.9$ were obtained using 10^5 independent Monte Carlo trials, for sample sizes $N = 3$ and $N = 6$. The first stage of the two-stage method is fixed to have a 99% acceptance rate ($\alpha = 0.01$) to avoid significant false alarms.

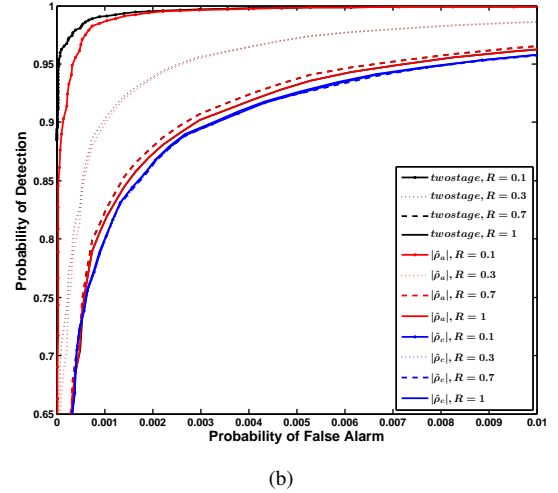
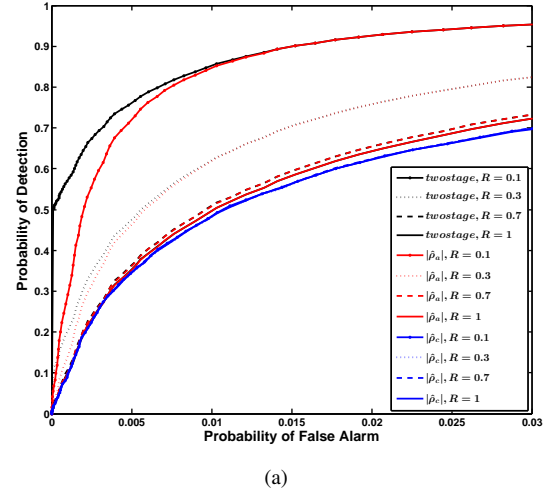


Fig. 3: Simulated ROC curves comparing the performance of two-stage method, $|\hat{\rho}_a|$ and $|\hat{\rho}_c|$ for variance ratios R of 0.1, 0.3, 0.7, and 1, with sample sizes of (a) $N = 3$ and (b) $N = 6$.

Figs. 3 (a) and (b) show the ROC curves for the change detection methods with varying variance ratios R and sample sizes of $N = 3$ and $N = 6$, respectively. The two-stage method is plotted in black,

$|\hat{\rho}_c|$ is denoted in blue, and $|\hat{\rho}_a|$ is represented with a red line.

We first compare the performance of using $|\hat{\rho}_c|$ vs. $|\hat{\rho}_a|$. Our empirical studies indicate that the change detection with $|\hat{\rho}_a|$ outperforms the change detection using $|\hat{\rho}_c|$, not only when the true underlying variances are equal, but also when they are far apart. Notice the performance of the change detection using $|\hat{\rho}_a|$ increases as R gets further away from one, implying a deviation from the underlying assumption leads to an improvement in change detection.

Next, we compare the change detection performance between the two-stage method and $|\hat{\rho}_a|$. Since the two-stage method uses the intensity change detector in the first stage, and $|\hat{\rho}_a|$ in the second stage, the two-stage method curve converges with that of $|\hat{\rho}_a|$. The performance improvement of the two-stage method compared to $|\hat{\rho}_a|$ is especially prominent at low P_{FA} and low R . The additional intensity change detection step allows the two-stage method to detect the regions of low R which leads to a higher P_D at a limited P_{FA} compared to other methods.

A comparison of Figs. 3 (a) and (b) confirms that overall change detection performance increases with N , and that, as expected with larger sample sizes, the curves tend toward unity.

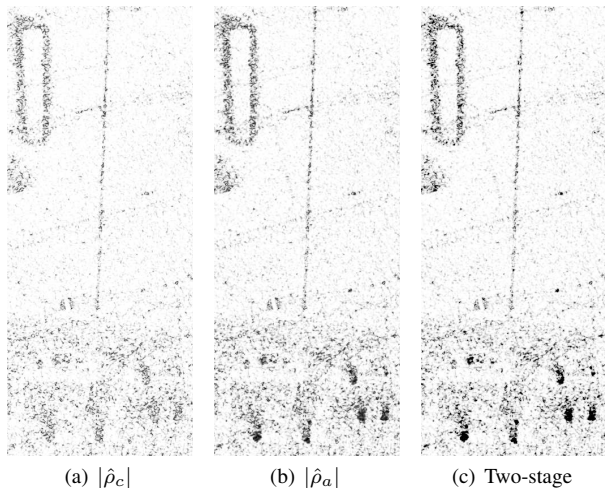


Fig. 4: SAR change detection images formed with $N = 5$, with (c) showing highest overall contrast.

To test this hypothesis, we form a CCD image using each of the methods. Again, the first stage of the two-stage method is fixed to 99% acceptance rate. The output of the consecutive second stage is shown as a resulting image. Notice in Fig. 4 (a) with $|\hat{\rho}_c|$, the car displacement changes are indistinguishable from the false alarms. However, Fig. 4 (b) with $|\hat{\rho}_a|$ clearly differentiates the car displacement changes. Fig. 4 (c) with the two-stage method further improves the result from $|\hat{\rho}_a|$ by emphasizing the large-scale changes.

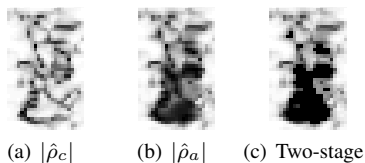


Fig. 5: Corresponding close-up view of a car displacement in a parking lot in Fig. 4, with (c) showing the highest contrast

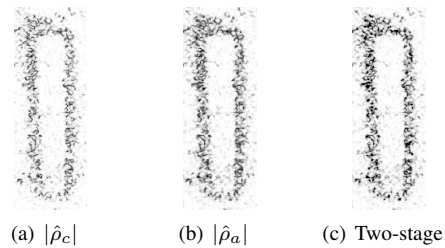


Fig. 6: Corresponding close-up view of footprints on a race track in Fig. 4, again with (c) showing the highest contrast

Smaller portions of Fig. 4 are shown to further illustrate the difference between the three methods in the regions of unequal variance in Fig. 5 and nearly equal variance in Fig. 6. Fig. 5 shows the zoom-in view of a car displacement change. Notice the center of the car displacement using $|\hat{\rho}_c|$ is hollow, making it difficult to identify as an object displacement change. However, the result from $|\hat{\rho}_a|$ fills in the hollow gap, and the two-stage method enhances the result of $|\hat{\rho}_a|$. Figs. 6 indicate footprints. As we expected a minor improvement from using $|\hat{\rho}_a|$ when $R = 1$, we observe a contrast enhancement in using $|\hat{\rho}_a|$ or the two-stage method compared to using $|\hat{\rho}_c|$. In regions of both large and small scale change, the two-stage method yields the highest contrast among the three techniques.

5. CONCLUSIONS

In this work, we have introduced a change detector based on two test statistics for SAR. This method is based on the use of the non-coherent intensity change statistic \hat{R} using a sample variance ratio followed by the coherent change statistic $|\hat{\rho}_a|$ which assumes equal population variances. The proposed method not only has superior change detection performance over the current state-of-the-art change detector $|\hat{\rho}_c|$, but also over either \hat{R} or $|\hat{\rho}_a|$, alone. We investigated the superior performance of the two-stage detector compared to other detectors in terms of ROC curves and visual inspection of the resulting CCD images. Comprehensive analytic evaluation of the proposed technique is currently under way.

6. REFERENCES

- [1] M. Preiss, D.A. Gray, and N.J.S. Stacy, "Detecting scene changes using synthetic aperture radar interferometry," *IEEE Trans. Geosci. Remote Sensing*, vol. 44, pp. 2041–2054, 2006.
- [2] T. Berger, "On the correlation coefficient of a bivariate, equal variance, complex Gaussian sample," *Ann. Math. Stat.*, vol. 43, pp. 2000–2003, 1972.
- [3] R. Touzi and A. Lopes, "Statistics of the stokes parameters and of the complex coherence parameters in one-look and multilook speckle fields," *IEEE Trans. Geosci. Remote Sensing*, vol. 34, pp. 764–773, 1996.
- [4] M. Cha, R.D. Phillips, and P.J. Wolfe, "Test statistics for synthetic aperture radar coherent change detection," in *IEEE SSP Workshop*, 2012.
- [5] T. Medkour and A.T. Walden, "A variance equality test for two correlated complex gaussian variables with application to spectral power comparison," *IEEE Trans. Signal Process.*, vol. 55, pp. 881–888, 2007.